

S & M 0769

# Development of Uracil and 5-Fluorouracil Sensors Based on Molecularly Imprinted Polymer-Modified Hanging Mercury Drop Electrode

Bhim Bali Prasad\*, Shrinkhala Srivastava,  
Khushaboo Tiwari and Piyush Sindhu Sharma

Analytical Division, Department of Chemistry, Faculty of Science,  
Banaras Hindu University, Varanasi 221005, India

(Received September 5, 2008; accepted January 14, 2009)

**Key words:** voltammetric sensor, uracil, 5-fluorouracil, molecularly imprinted polymerisation, differential pulse cathodic stripping voltammetry

Molecularly imprinted polymers (MIPs), imprinted for uracil and 5-fluorouracil, were used in the development of electrochemical sensors for selective and sensitive analysis of uracil and 5-fluorouracil in aqueous and blood plasma samples. The same MIP motif prepared from melamine and chloranil precursors was used for both analytes as a coating material for modification of a hanging mercury drop electrode (HMDE) by a drop-coating method using dimethylformamide casting solution. This revealed the imprinting versatility of the imprinted polymer, where binding events for both analytes in aqueous environments were transduced into their respective differential pulse, cathodic stripping voltammetric signals with high sensitivity and without any false positive results owing to nonspecific sorptions, interferences and cross-reactivities. The limits of detection ( $3\sigma$ ) for uracil and 5-fluorouracil were found to be as low as 0.34 and 0.26 ng mL<sup>-1</sup>, respectively, which enable substantial sensitivity in the diagnosis of uracil-disorders and fluoropyrimidine toxicity in patients.

## 1. Introduction

The levels of nucleosides and their metabolic compounds have been proposed as markers for diagnosis of cancers, AIDS, disease progress, and therapy responses. Inherited purine and pyrimidine disorders may be associated with inborn errors of metabolism (IEM), which shows significant variations in biological fluids with respect to normal values. Therefore, the chemical analysis of biological fluids for the screening of IEM is crucial to achieving prenatal diagnosis. Uracil (Ura), which is a pyrimidine base, is associated with such types of IEM particularly at the 0.25 µg mL<sup>-1</sup> concentration level in patients suffering from dihydropyrimidine dehydrogenase (DPD) deficiency and

---

\*Corresponding author: e-mail: prof.bbpd@yahoo.com

Canavan disease.<sup>(1)</sup> Basal plasma Ura concentration ranges from 3 to 30 ng mL<sup>-1</sup>. Another pyrimidine base, 5-fluorouracil (5FU), is an important drug, widely used in combination with other drugs, in the treatment of various cancers. There exists a strong correlation of Ura and 5FU with DPD as both pyrimidines are catabolised by the same pathway to dihydrouracil and dihydrofluorouracil. Also, there is an apparent relationship between 5FU plasma levels and their known toxicity. Since toxicity and response rates clearly correlate with 5FU plasma levels in different administration schedules, drug level measurement in plasma can help monitor 5FU doses and develop optimum procedure for drug administration. Since 5FU has a narrow therapeutic index and short half lifetime, the level of 5FU could be very low, in the range between 0.26 and 13 µg mL<sup>-1</sup>, upon being metabolised within 2 to 48 h after drug administration.

The literature revealed various chronic problems, such as longer response time, electrode fouling, electrode regeneration and large consumption of eco-unfriendly solvents associated with tedious instrumental techniques, namely, voltammetry,<sup>(2,3)</sup> chromatography,<sup>(4)</sup> capillary electrophoresis,<sup>(5)</sup> and spectroscopy,<sup>(6)</sup> employed for Ura analysis. Although solid electrodes were reportedly successful for trace level analysis (not ng mL<sup>-1</sup> range),<sup>(7)</sup> sensors and biosensors for Ura and 5FU have been paid little attention.<sup>(8-10)</sup> Furthermore, microbiological assays,<sup>(11)</sup> particularly for 5FU detection, appeared to be equivocal in cases where patients were receiving antibiotics. Other methods of 5FU analysis, viz., solid phase extraction,<sup>(12)</sup> gas chromatography-mass spectrometry (GC-MS),<sup>(13)</sup> high performance liquid chromatography (HPLC),<sup>(14)</sup> and cathodic stripping voltammetry,<sup>(15)</sup> require highly sophisticated equipment. These methods are not amenable to a rapid and routine clinical assay owing to the polar nature of 5FU and inevitable sample treatment (extraction, deproteinisation and derivatisation etc.) before analysis.

A few approaches to obtaining affinity matrices have been reported on the basis of most burgeoning techniques of molecular imprinting for Ura<sup>(16-25)</sup> and 5FU.<sup>(26-28)</sup> However, the cross-reactivity between Ura and 5FU, especially in high polarity media, could not be ruled out.<sup>(26)</sup> It should be further noted that none of the MIPs, reported to date, have been utilised for sensor development, primarily because of the transduction challenges yet to be resolved.

In our laboratory, we have prepared a novel MIP format, poly(melamine-co-chloranil), involving melamine and chloranil as precursors and studied its imprinting versatility with a number of biomolecules.<sup>(29,30)</sup> The present work is focused on exploring the isolation and quantitative identification abilities of this MIP when two structurally identical pyrimidine bases (Ura and 5FU) are simultaneously present in a blood plasma sample. This would reveal the cross-selectivity of two different analytes imprinted individually with the same MIP and direct sensing efficacy in blood plasma, without performing tedious sample pretreatment that often leads to inaccuracies in trace level measurements. Keeping abreast of the usual limitations of MIPs such as long response time, slow mass transfer, nonspecific binding, and electrode fouling with solid sensors, the present investigation is also directed towards addressing these constraints by invoking the concept of surface-attached rebinding and transduction on MIP-modified electrodes individually developed for Ura and 5FU.

## 2. Experimental Procedure

### 2.1 Materials and reagents

The reagents melamine (mel), chloranil (chl), uracil (Ura), 5-fluorouracil (5FU), and other chemicals were purchased from Loba Chemie, India, Otto kemi, India and Spectrochem, India. All chemicals were of analytical grade. The solvent dimethylformamide (DMF) was of HPLC quality. The stock standard solutions of Ura and 5FU were prepared by dissolving 0.0125 g of analyte in 25 mL of water (demineralised triple distilled water, conductivity range  $0.06\text{--}0.07\times 10^{-6}$  S  $\text{cm}^{-1}$ ). The working solutions of analytes were prepared by appropriate dilutions and pH was adjusted to 7.0 by adding aqueous solutions of 0.01 M NaOH and HNO<sub>3</sub>.

### 2.2 Equipment

All voltammetric measurements were carried out with a polarographic analyser/stripping voltammeter (Model 264 A EG & G Princeton Applied Research, USA) in conjunction with an X-Y recorder (PAR Model RE 0089). The three-electrode cell of a 303A static mercury drop unit (EG & G Princeton Applied Research) consisted of an HMDE (surface area 0.0092 cm<sup>2</sup>), a saturated Ag/AgCl electrode with a porous Vycor frit, and a platinum wire electrode as working, reference and auxiliary electrodes, respectively. Varian 3100 FT/IR (USA), and JEOL AL 300 FT NMR (Japan) were used for IR and NMR studies, respectively. Scanning electron microscopy (SEM) images were recorded using the XL-20 model (Philips, Holland).

### 2.3 Molecularly imprinted polymer preparation

The preparation and characterisation of Ura and 5FU imprinted polymers, abbreviated hereafter as MIP(Ura) and MIP(5FU), and corresponding nonimprinted polymers, NIP(Ura) and NIP(5FU), were performed on the basis of the conventional bulk condensation polymerisation procedure reported earlier.<sup>(29)</sup> Normally, in a single batch, equimolar DMF solutions of mel (1.26 g/10 mL) and chl (2.46 g/10 mL) were mixed together and heated at ca. 160°C for 1 h followed by the addition of template(s) (1.1209 g of Ura/1.308 g of 5FU dissolved in 10 mL of DMF) into the reaction mixture. The polymeric-template adduct, in the form of DMF slurry, was obtained after the complete evaporation of DMF. For complete template removal from MIPs, 0.1 M HCl (number of extractions 10, shaking time 10 min, 1.5 mL portions) and 50% (v/v) MeOH-H<sub>2</sub>O (number of extractions 10, shaking time 10 min, 2.5 mL portions) were found to be the most suitable extractants for Ura and 5FU, respectively. Similarly, NIP was prepared with mel and chl precursors in DMF in the absence of template(s). Whereas analyte binding in MIP(Ura) (Fig. 1(a)) and MIP(5FU) (Fig. 1(b)) proceeded through multiple hydrogen-bonding interactions in DMF (porogen), the rebinding process typically followed similar interactions with the exclusion of water between hydrophobic MIP and analyte moieties in aqueous environments. Cross-linkage in polymer preparations was deliberately avoided in order to allow better accessibility of binding sites, without any steric compression.

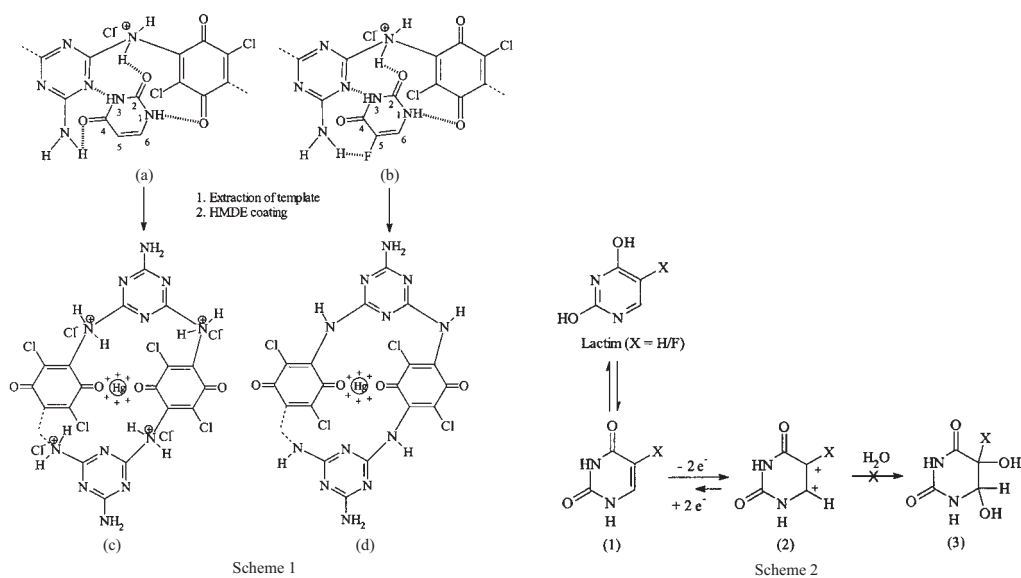


Fig. 1. (a) and (b) represent binding mechanisms for Ura and 5FU, respectively, with MIP. (c) and (d) represent MIP(Ura)- and MIP(5FU)-coated HMDE sensors for Ura and 5FU, respectively (Scheme 1). Mechanism of electrocatalytic oxidation of Ura and 5FU in aqueous medium (pH 7.0) (Scheme 2).

#### 2.4 Voltammetric method

Differential pulse, cathodic stripping voltammetry (DPCSV) runs were recorded following the reported procedure.<sup>(29)</sup> For modifying the HMDE, with optimised MIP concentrations of MIP(Ura) ( $600 \mu\text{g mL}^{-1}$ ) and MIP(5FU) ( $400 \mu\text{g mL}^{-1}$ ), directly in a voltammetric cell, the HMDE was submerged in respective MIP-DMF solutions at +0.4 and +0.3 V (relative to Ag/AgCl) for Ura and 5FU, respectively, for 120 s in all measurements. Another cell containing an aqueous solution of the test analyte (in the absence of any supporting electrolyte) was brought under the modified electrode for an optimised accumulation period ( $t_{\text{acc}}$ ) of 120 s under quiescent conditions. After 15 s equilibration time, DPCSV runs were recorded (scan rate  $10 \text{ mVs}^{-1}$ , pulse amplitude 25 mV) from +0.4 to  $-1.2 \text{ V}$  for Ura and from +0.3 to  $-0.7 \text{ V}$  for 5FU at room temperature ( $25 \pm 1^\circ\text{C}$ ). All runs for each concentration of test analyte and subsequent quantification (standard addition method) were always carried out with fresh mercury drops duly modified with MIP. The deaeration of the cell content was not performed as dissolved oxygen did not interfere with the stripping voltammetry in the present instance. Moreover, there may exist some diminishing effects of pyrimidine derivatives on oxygen waves.<sup>(31)</sup> All measurements were also carried out using NIP-modified HMDEs, under identical DPCSV conditions.

### 3. Results and Discussion

#### 3.1 Sensor development

In this work, the procedure for sensor development was mainly adopted from our previous work,<sup>(29,30)</sup> where the drop coating approach of HMDE surface modification with MIP-DMF solution was used to obtain a controlled and reproducible film thickness. Since MIP-DMF solution was stable, no deformation of cavities after solvent evaporation was possible, as confirmed earlier.<sup>(29)</sup> The modified HMDE with a tiny hanging mercury drop was the most preferred choice to ensure an ultrathin layer coating, despite the fact that the use of mercury is not ecofriendly. Furthermore, an ultrathin layer of polymer coating over the solid electrodes appeared to be cumbersome, and current response was also limited owing to the restricted mass transfer. However, HMDE modification could be considered better for ensuring the absolute absence of problems related to film thickness reproducibility, electrode fouling, and critical regeneration, as encountered with solid electrodes. Since every voltammetric measurement was accomplished with a new hanging mercury drop freshly modified with MIP, a high level of sensitivity was achieved in this work. The porosity and permeability of the film and its thickness reproducibility over the mercury drop were evident as three concurrent DPCSV runs with a fresh HMDE, duly modified with optimised polymer concentrations ( $600 \mu\text{g mL}^{-1}$  MIP(Ura),  $400 \mu\text{g mL}^{-1}$  MIP(5FU)), always resulted in precise and accurate results. The firm adherence of MIP film at the positively charged [+0.4 V (Ura), +0.3 V (5FU) vs Ag/AgCl] HMDE surface primarily involved coulombic interactions between preanodised mercury drop and electron-rich precursor functionalities [chl  $-\text{C}=\text{O}$ , mel ring nitrogen in the case of MIP(Ura) and chl  $-\text{C}=\text{O}$ , mel ring nitrogen, mel  $2^\circ$  amine in the case of MIP(5FU)] (Figs. 1(c) and 1(d)). In contrast to Fig. 1(c) where entwined cationic centres ( $-\text{NH}_2^+\text{Cl}^-$ ) remained electroneutral during template retrieval by 0.1 M HCl, all cationic centres turned out to be  $2^\circ$  amines, as shown in Fig. 1(d), on template retrieval using 50% (v/v) MeOH- $\text{H}_2\text{O}$ . In both MIPs, in the absence of any cross-linkage, binding sites were outwardly exposed to recapture the template. The electrode preanodisation actually helped electrocatalytic oxidation to transduce a binding event into a corresponding DPCSV signal. The favoured hydrogen bondings in aqueous media between the water-compatible MIP and the template resulted in rebinding mainly dependent on the hydrophobic behavior of the MIP and analytes (Ura and 5FU) under study. Hydrophobicity reinforces hydrogen bondings, with the exclusion of water between the guest and the host, in the rebinding process.

The hydrophobically driven hydrogen bondings in both cases of MIPs were confirmed from IR and NMR spectra. A routine sample for proton NMR on a scanning 300 MHz instrument consisted of about 5–20 mg of the polymer in about 0.4 mL of deuterated DMSO in a 5-mm-outer diameter glass tube. For IR study, the imprinted polymers were examined either as a mull or a pressed disk. A mull is prepared by thoroughly mixing 2–5 mg of bulk polymer with 1–2 drops of Nujol and is examined as a thin film between flat salt plates. In the pellet (pressed-disk) technique, the bulk polymer sample (0.5–1.0 mg) is intimately mixed with approximately 100 mg of dry, powdered KBr and then pressed with special dies under a pressure of 10,000–15,000 psi into a transparent disk. Both

NMR and IR spectra showed respective peak shiftings of the bonding functionalities in a reversible manner, on account of multiple hydrogen bondings during template recapture and the disruption of hydrogen bonds on template retrieval, as given below:

- MIP(Ura)

IR (Nujol): N<sub>1</sub> proton of Ura, shifting from 3,500 to 3,400 cm<sup>-1</sup> downward; N<sub>3</sub> proton of Ura, shifting from 3,400 to 3,350 cm<sup>-1</sup> downward; mel-amine, shifting from 3,350 to 3,211 cm<sup>-1</sup> downward; chl -C=O, shifting from 1,630 to 1,580 cm<sup>-1</sup>; -C=O (C<sub>4</sub>) of Ura, shifting from 1,714 to 1,635 cm<sup>-1</sup> downward; -C=O (C<sub>2</sub>) of Ura, shifting from 1,650 to 1,580 cm<sup>-1</sup> downward; -NH<sub>2</sub><sup>+</sup>Cl<sup>-</sup>, shifting from 2,934 to 2,856 cm<sup>-1</sup> downward; -CN stretching of melamine, shifting from 1,460 to 1,377 cm<sup>-1</sup> downward.

NMR (DMSO-d<sub>6</sub>): N<sub>1</sub> proton of Ura, shifting from 10.83 to 10.86 ppm downfield; N<sub>3</sub> proton of Ura, shifting from 11.01 to 11.10 ppm downfield; mel-amine, shifting from 3.30 to 3.35 ppm downfield; proton of 2° amine salt, shifting from 8.0 to 8.30 ppm downfield.

- MIP(5FU)

IR (KBr): N<sub>1</sub> proton of 5FU, shifting from 3,134 to 3,050 cm<sup>-1</sup> downward; N<sub>3</sub> proton of 5FU, shifting from 3,067 to 3,237 cm<sup>-1</sup> upward; mel-amine, shifting from 3,330 to 3,398 cm<sup>-1</sup> upward; chl -C=O, shifting from 1625 to 1580 cm<sup>-1</sup> downward; broad peak for -C=O (C<sub>2</sub>), shifted from 1,723 to 1,700 cm<sup>-1</sup> downward and merged with unshifted -C=O (C<sub>4</sub>) peak at 1,660 cm<sup>-1</sup>; -CN stretching, shifting from 1,380 to 1,469 cm<sup>-1</sup> upward; -C-F stretching, shifting from 1,503 to 1,469 cm<sup>-1</sup> downward. Peak for 2° amine in MIP(5FU) at 3,207 cm<sup>-1</sup> followed by the disappearance of peak of 2° amine salt at 3,000 cm<sup>-1</sup>.

NMR (DMSO-d<sub>6</sub>): N<sub>1</sub> proton of 5FU, shifting from 10.7 to 10.77 ppm downfield; N<sub>3</sub> proton of 5FU, shifting from 11.45 to 11.50 ppm downfield; mel-amine, shifting from 3.23 to 3.37 ppm downfield; along with the appearance of peak corresponding to 2° amine proton at 2.8 ppm.

In MIP(5FU), the -C=O (C<sub>4</sub>) remained intact at 1660 cm<sup>-1</sup> without accepting a hydrogen bond with mel-NH<sub>2</sub>, unlike in MIP(Ura). This is due to the presence of a fluorine atom at the C<sub>5</sub> position, lowering the ability of the neighbouring function -C=O at the C<sub>4</sub> position to accept a hydrogen bond.<sup>(32)</sup> The fluorine atom itself was involved in hydrogen bonding with mel-amine (Fig. 1(b)). This inculcated a contrastive discriminating ability in the memory of the same MIP motif employed for the molecular recognition of Ura and 5FU.

The surface morphologies of the Ura- and 5FU-imprinted MIPs were studied by SEM at a high magnification of 3,699. First of all, on an Al stub, a silver glue film of approximately μm thickness was formed to make the mounted polymer sample (0.1 mg) conducting and then a convergent beam of electrons was bombarded over it. The SEM image was detected as secondary electron emission. As evident from Fig. 2, the polymers were more porous and had a rough morphology (rather than microparticles with small cavities). While MIP(Ura) had small cavities between larger ones, MIP(5FU) showed a compact clusterous appearance with larger pores of cavities and wide openings.

### 3.2 Voltammetric behaviour

The film-entrapped Ura and 5FU were readily preoxidised at their respective preanodised electrodes after accumulation. This subsequently, after 15 s equilibration

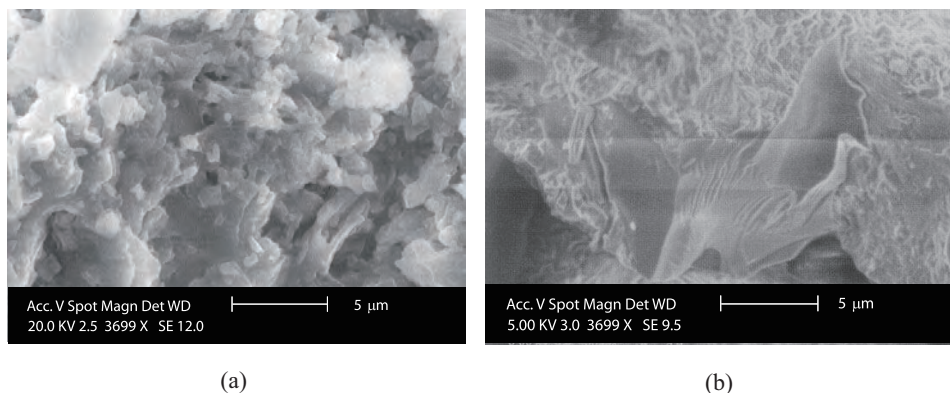


Fig. 2. SEM images of (a) MIP(Ura) and (b) MIP(5FU).

time, demonstrated a broad cathodic stripping peak ( $I_c$ ) at  $-0.2$  V (Ura) and  $-0.25$  V (5FU) at a scan rate of  $10$   $\text{mVs}^{-1}$ , followed by an ill-defined anodic peak ( $I_a$ ) on reverse scan in cyclic voltammetry (CV). The observed shifts towards a more negative potential at higher scan rates (Fig. 3) could be considered as indications of hydrophobically induced hydrogen bondings of Ura/5FU molecules in MIP cavities, which required a relatively high energy for cathodic stripping. The slightly easier stripping at low scan rates could be attributed to the disruption of hydrogen bonds, as a consequence of water competence and thereby the hydration of the oxidised form of Ura/5FU, at a sufficient time in a hydrophobic environment. The appearance of an adsorption prepeak preceding the diffusion peak ( $I_c$ ) is attributed to the strong adsorption of the stripping product (presumably target analyte in lactum form), notwithstanding the known irreversibility of Ura and 5FU oxidations.<sup>(7,33)</sup> The observed quasi-reversibility [ $\Delta E_p$  ( $E_{pc} - E_{pa}$ ) =  $250$  mV (Ura),  $275$  mV (5FU), scan rate  $10$   $\text{mVs}^{-1}$ ] of the electrode process, despite peak shifting on cathodic scan with increasing scan rate and analyte concentration (Fig. 3), revealed the presence of a strong electrocatalytic effect in the MIP-modified layer over the HMDE surface in the case of both analytes.<sup>(34)</sup> While the electrocatalytic effect facilitated the re-reduction in cathodic scan, the strong adsorption of the reduction product at the electrode surface appeared as a restricting anodic peak ( $I_a$ ) with an increase in analyte concentration on reverse scan. The electron-transfer mechanism (Scheme 2, Fig. 1) reported earlier<sup>(7)</sup> is apparently most plausible for explaining the aforementioned CV-stripping behavior. Accordingly, the encapsulated target analytes (Ura/5FU) (1) were initially electrochemically oxidised in a  $2e^-$  process to give a highly unstable dicationic species (2). This species later preferred to go back to (1) on cathodic stripping under the electrocatalytic effect rather to the restricted hydration as a consequence of the hydrophobic domain of the MIP-template adduct. The dicationic oxidation product (2) remained strongly adsorbed during cathodic scan under electrostatic interaction. The more negative shift in the peak potential of 5FU than that in the case of Ura corroborates the electron donating mesomeric effect of halogen at the  $C_5$  position along the  $-C=C-$  double bond making reduction more difficult than that of Ura.<sup>(7)</sup> The charge transport in

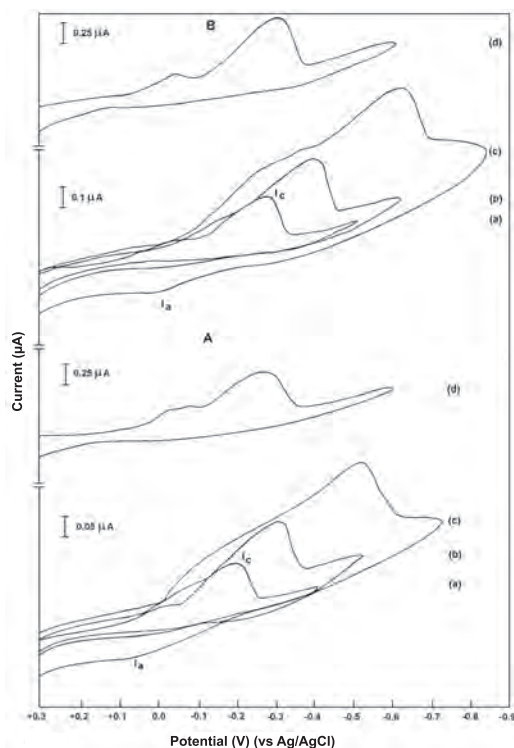


Fig. 3. A: Typical cathodic stripping cyclic voltammograms of Ura with MIP(Ura)-modified HMDE (runs (a)–(c) recorded at scan rates of 10, 20, and 50  $\text{mVs}^{-1}$ , respectively, for Ura concentration of  $0.0244 \mu\text{g mL}^{-1}$ , and run (d) recorded at scan rate of 10  $\text{mVs}^{-1}$  for Ura concentration of  $28.30 \mu\text{g mL}^{-1}$ ). B: Typical cathodic stripping cyclic voltammograms of 5FU with MIP(5FU)-modified HMDE (runs (a)–(c) recorded at scan rates of 10, 20, and 50  $\text{mVs}^{-1}$ , respectively, for 5FU concentration of  $0.0099 \mu\text{g mL}^{-1}$ , and run (d) recorded at scan rate of 10  $\text{mVs}^{-1}$  for 5FU concentration of  $14.56 \mu\text{g mL}^{-1}$ ). MIP (Ura) and Ura accumulation potential:  $+0.4 \text{ V}$  (vs Ag/AgCl); MIP(5FU) and 5FU accumulation potential:  $+0.3 \text{ V}$  (vs Ag/AgCl); [MIP(Ura)]:  $600 \mu\text{g mL}^{-1}$ ; [MIP(5FU)]:  $400 \mu\text{g mL}^{-1}$ ; deposition time of polymer ( $t_d$ ): 120 s; accumulation time of analyte ( $t_{acc}$ ): 120 s; pH 7.0.

the present case apparently involved an electron hopping process between redox centres incorporated in an MIP film (homogeneous electron transfer) and the positively charged electrode surface (heterogeneous electron transfer). As is evident from the negative potential shift in  $I_c$  (Fig. 3), there seems to be difficulty in the stripping of imprint molecules (oxidised form) at higher concentrations. Consequently, the cathodic stripping current response was restricted in comparison with that for lower analyte concentrations. The reduction in current response at higher analyte concentrations can also be accorded to the high diffusion barrier for electron transport across the film layer onto the modified HMDE.



Ura is typically sensed as a doubly charged anion (predominant at pH 7.0 in tautomeric form),<sup>(35)</sup> during rebinding in aqueous environments. This was feasible under the electrostatic interaction with a polymeric skeleton consisting of interspersed cationic charges ( $-\text{NH}_2^+\text{Cl}^-$ ), in addition to hydrophobic hydrogen bondings. However, 5FU exclusively involved hydrophobically induced hydrogen bondings in aqueous environments despite its dianionic behavior at pH 7.0. Whatsoever the case, the adsorbed lactim tautomerised to a more stable lactam (2-oxo-4-oxo form at pH 7),<sup>(36)</sup> at the activated electrode surface to render an apparent tenacity for its anodic oxidation. The effect of pH on the response of both sensors was examined. The respective current-pH profiles indicated an optimum pH of 7.0 for a maximum current response. The lower response at extreme pH values may be due to the precipitation ( $\text{pH} \leq 6$ ) and hydrolysis ( $\text{pH} \geq 8$ ) of the analyte studied.

The DPCSV runs of Ura and 5FU using corresponding sensors are shown in Fig. 4. The difficult stripping at higher concentrations (Figs. 4A and 4B (d, e)), such as in CV, is reflected by the slight cathodic shifting of peak potentials, as compared with that at lower concentrations (Figs. 4A and 4B (a, b)), and by the restricted DPCSV response. The rectilinear symmetries of peak currents observed for both cases of analytes were masked in the beginning of the peak formation, owing to the emergence of an ill-defined broader pre-adsorption peak. However, all DPCSV runs were easily quantifiable than CV by spiking the cell content with an authentic amount.

### 3.3 Optimisation of analytical parameters

Both MIP(Ura)- and MIP(5FU)-modified sensors were examined to determine maximum DPCSV currents for the test analytes Ura and 5FU, respectively, in a neutral aqueous medium. This was performed via two types of saturation experiment: (i) DPCSV measurement with an increase in the concentration of MIP used in electrode coating (analyte concentration fixed) and (ii) DPCSV measurement with an increase in template (analyte) concentration (MIP concentration fixed). The corresponding results are summarised in Table 1. Both the operational parameters  $t_{\text{acc}}$  and  $E_{\text{acc}}$  used in the binding event were the same as those adopted for the MIP coating of HMDE. The DPCSV for Ura recorded at  $E_{\text{acc}} \leq +0.3$  V (vs Ag/AgCl) yielded almost constant currents ( $\sim 0.125$   $\mu\text{A}$ ) but showed a significant rise in current when the modified electrode was preanodised at +0.4 V. This indicated the favored electrostatic interaction between Ura (dianionic (lactim) form) and MIP during the rebinding process. The subsequent tautomerisation of Ura into a stable diketo (lactam) form favored oxidation under the electrocatalytic activity of the preanodised HMDE surface. On the other hand, the optimum potential for polymer coating and 5FU rebinding was found to be +0.3 V, which appeared to be critical to withhold film and upheld 5FU oxidation. Any potential higher or lower than +0.3 V might have caused the prompt destabilisation of the MIP-5FU adduct. This was due to the facilitated oxidation and thereby electrostatic repulsion between the positively charged electrode and the oxidised 5FU (dicationic form), under the mesomeric effect of fluorine ( $\text{C}_5$ ). As far as MIP concentration was concerned for electrode coating, Ura detection required a higher MIP concentration than 5FU detection. This was ostensibly because of high positive charge density along the parent polycation chain required for exerting the electrostatic rebinding of the Ura (lactim form) molecule.

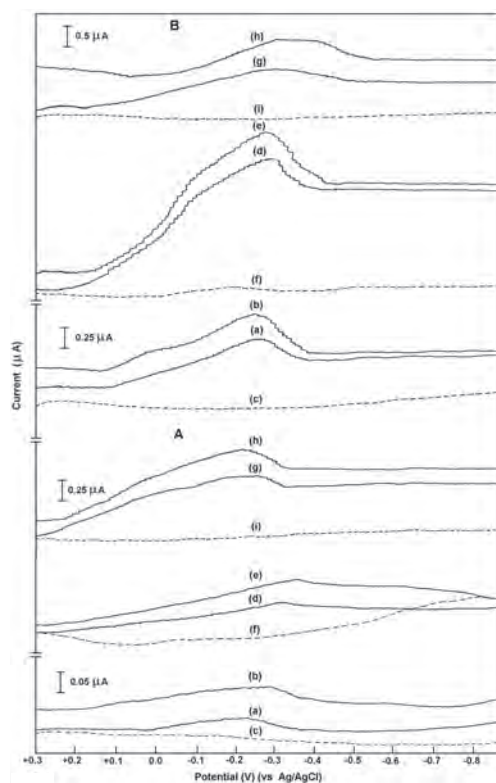


Fig. 4. A: DPCSV measurement of Ura with MIP(Ura)-modified HMDE in aqueous samples [Ura concentration ( $\mu\text{g mL}^{-1}$ ): (a) 0.00299; (b) 0.00596; (d) 14.56; and (e) 28.30]; DPCSV with NIP-modified HMDE [Ura concentration ( $\mu\text{g mL}^{-1}$ ): (c) 0.00099 and (f) 9.80], DPCSV measurement with MIP-modified HMDE in blood plasma samples [Ura concentration ( $\mu\text{g mL}^{-1}$ ): (g) 0.02512 and (h) 0.03966]; DPCSV with NIP-modified HMDE [Ura concentration ( $\mu\text{g mL}^{-1}$ ): (i) 0.00049]. B: DPCSV measurement of 5FU with MIP(5FU)-modified HMDE in aqueous samples [5FU concentration ( $\mu\text{g mL}^{-1}$ ): (a) 0.00942; (b) 0.01332; (d) 20.15; and (e) 29.20]; DPCSV with NIP-modified HMDE [5FU concentration ( $\mu\text{g mL}^{-1}$ ): (c) 0.00942 and (f) 29.20], DPCSV measurement with MIP-modified HMDE in blood plasma samples [5FU concentration ( $\mu\text{g mL}^{-1}$ ): (g) 0.01239 and (h) 0.01683]; DPCSV with NIP-modified HMDE [5FU concentration ( $\mu\text{g mL}^{-1}$ ): (i) 0.01239]. The other conditions are the same as those in Fig. 3.

Table 1  
Operational analytical parameters optimised at MIP-modified HMDE sensors.

Optimised parameters	Templates	
	Ura	5FU
MIP concentration ( $\mu\text{g mL}^{-1}$ )	600	400
MIP deposition time ( $t_d$ )	120 s	120 s
pH of the test solution	7.0	7.0
Preanodisation potential/analyte accumulation potential ( $E_{\text{acc}}$ (V) vs Ag/AgCl)	+0.4	+0.3
Analyte accumulation time ( $t_{\text{acc}}$ )	120 s	120 s

An excess MIP amount compared with the respective optimised value(s) in both Ura and 5FU detections was avoided, in view of the relatively thick film coating. The thick film might show a slow mass transfer and a decreasing partition coefficient of the test analyte resulting in a marked decrease in DPCSV current.

In the present investigation, the problem of false positive results due to nonspecific bindings was not encountered as the corresponding nonimprinted polymer-modified HMDE did not respond to any binding of Ura and 5FU at any concentration level (Figs. 4A and 4B (c, f, i)). The actual problem was encountered during the early saturation of the current response in the lower concentration region. This was probably because of the predominating hydrophobic environment causing multiple H-bonds between templates (Ura and 5FU) and the receptor cleft. Surprisingly, the average currents in the present work were observed to be on the orders of  $10^{-2}$   $\mu\text{A}$  (Ura) and  $10^{-1}$   $\mu\text{A}$  (5FU) in both concentrated as well as dilute ranges of analyte concentrations under the optimised operational conditions, for the reasons described in §3.2. Nevertheless, one may opt for either of the concentration regions because these yielded binding isotherms with excellent linearity between the cathodic peak current [ $I_{\text{PC}}$  ( $\mu\text{A}$ )] and the analyte concentration [ $C$  ( $\mu\text{g mL}^{-1}$ )] according to the following calibration equations: (For Ura analysis using MIP(Ura)-modified HMDE at 95% confidence level)

- Lower concentration range (0.00099–0.10873  $\mu\text{g mL}^{-1}$ );

$$I_{\text{PC}} = (7.583 \pm 0.036)C + (0.00014 \pm 0.00018), \nu = 0.99, n = 8 \quad (1)$$

- Higher concentration range (0.99–45.45  $\mu\text{g mL}^{-1}$ );

$$I_{\text{PC}} = (0.01485 \pm 0.00008)C + (0.00007 \pm 0.00004), \nu = 0.99, n = 6 \quad (2)$$

(For 5FU analysis using MIP(5FU)-modified HMDE at 95% confidence level)

- Lower concentration range (0.00099–0.03614  $\mu\text{g mL}^{-1}$ );

$$I_{\text{PC}} = (39.026 \pm 0.004)C + (0.00365 \pm 0.00023), \nu = 0.99, n = 7 \quad (3)$$

- Higher concentration range (0.49–32.27  $\mu\text{g mL}^{-1}$ );

$$I_{\text{PC}} = (0.065 \pm 21 \times 10^{-7})C + (0.0005 \pm 0.0004), \nu = 0.99, n = 8 \quad (4)$$

The minimum detectable values, i.e., the limits of detection (LODs) for both analytes in dilute aqueous solutions, computed following a standard procedure,<sup>(37)</sup> were as follows:

- LOD (Ura) = 0.34  $\text{ng mL}^{-1}$  ( $3\sigma$ ,  $RSD = 0.6\%$  between three sets of LOD data)
- LOD (5FU) = 0.26  $\text{ng mL}^{-1}$  ( $3\sigma$ ,  $RSD = 0.3\%$  between three sets of LOD data)

### 3.4 Cross-selectivity study

The most appealing feature of the present investigation is the excellent imprinting effect, which showed a perfect discrimination between the two stereospecifically identical templates, Ura and 5FU. Although the MIPs for Ura and 5FU have the same

structural motif, the MIP(Ura)-modified electrode exclusively recognised Ura (not 5FU) and the MIP(5FU)-modified electrode exclusively recognised 5FU (not Ura) at all concentration levels in aqueous environments. Similarly both sensors were found to recognise their respective templates quantitatively in mixed solutions consisting of interferents at clinically relevant ratios, as shown in Table 2.

Table 2

Analytical results of DPCSV measurements of Ura and 5FU in water samples with interferents at MIP-modified HMDE.

Sample	Analyte concentration ( $\mu\text{g mL}^{-1}$ )	Determined value <sup>a</sup> (mean $\pm$ S.D.) ( $\mu\text{g mL}^{-1}$ with MIP- modified HMDE)	Recovery <sup>b</sup> (%)	Relative standard deviation (%) ( $n = 3$ )
Ura with interferents <sup>c</sup>	0.00474 (0.0474 5FU) <sup>d</sup>	0.00468 $\pm$ 0.00011	98.7	2.4
	0.00474 (0.0474 BA) <sup>d</sup>	0.00470 $\pm$ 0.00006	99.2	1.3
	0.00485 (0.02425 Hx) <sup>e</sup>	0.00476 $\pm$ 0.00014	98.1	2.9
	0.00490 (0.01471 Ad) <sup>f</sup>	0.0050 $\pm$ 0.000070	102.0	1.4
	0.00474 (0.0474 Cff) <sup>d</sup>	0.00475 $\pm$ 0.00020	100.2	4.2
	0.00495 (0.00495 Cy) <sup>g</sup>	0.00481 $\pm$ 0.00026	97.2	5.4
	0.00099 (0.99 UA) <sup>h</sup>	0.00099 $\pm$ 0.00001	100.0	1.0
	0.00495 (0.00495 Gu) <sup>g</sup>	0.00493 $\pm$ 0.00002	99.6	0.4
	0.010 (0.1 5FU, BA, Hx, Ad, Cff, Cy, UA, Gu each) <sup>d</sup>	0.01014 $\pm$ 0.00012	101.4	1.2
5FU with interferents <sup>c</sup>	0.0090 (0.09 Ura) <sup>d</sup>	0.00889 $\pm$ 0.00009	98.8	1.0
	0.0090 (0.09 BA) <sup>d</sup>	0.00898 $\pm$ 0.00007	99.8	0.8
	0.0090 (0.09 Hx) <sup>d</sup>	0.00875 $\pm$ 0.00037	97.2	4.3
	0.0090 (0.09 Ad) <sup>d</sup>	0.00926 $\pm$ 0.00053	102.9	5.7
	0.0090 (0.09 Cff) <sup>d</sup>	0.00894 $\pm$ 0.00010	99.3	1.1
	0.0090 (0.09 Cy) <sup>d</sup>	0.00896 $\pm$ 0.00037	99.6	4.1
	0.0090 (0.09 UA) <sup>d</sup>	0.00872 $\pm$ 0.00003	97.0	0.3
	0.0090 (0.09 Gu) <sup>d</sup>	0.00908 $\pm$ 0.00043	100.9	4.7
	0.0090 (0.09 AA) <sup>d</sup>	0.00885 $\pm$ 0.00033	98.3	3.7
	0.010 (0.1 Ura, BA, Hx, Ad, Cff, Cy, UA, Gu, AA each) <sup>d</sup>	0.00996 $\pm$ 0.00011	99.6	1.1

<sup>a</sup>Average of three replicate determinations ( $S/N = 3$ ) with fresh MIP-modified HMDE.

<sup>b</sup>Recovery: Amount of analyte determined/amount of analyte taken.

<sup>c</sup>Values in parentheses indicate concentrations ( $\mu\text{g mL}^{-1}$ ) of various interferents taken with test analyte in aqueous mixture solutions.

<sup>d</sup>Analyte: interferent concentration ratio (1:10)

<sup>e</sup>Analyte: interferent concentration ratio (1:5)

<sup>f</sup>Analyte: interferent concentration ratio (1:3)

<sup>g</sup>Analyte: interferent concentration ratio (1:1)

<sup>h</sup>Analyte: interferent concentration ratio (1:1000)

It is known that MIP recognition properties versus possible interferent compounds may change in the absence of a template molecule, which in most cases displaces other compounds from MIP-binding sites. For this reason, it is necessary to evaluate the possibility of having false positives due to interferents in the absence of a test analyte in a sample. Therefore, a parallel cross-reactivity study in the absence of a template was performed with some important purine and pyrimidine bases, viz., barbituric acid (BA), hypoxanthine (Hx), adenine (Ad), caffeine (Cff), cytosine (Cy), uric acid (UA), and guanine (Gu), along with ascorbic acid (AA), as major interferents (structures shown in Fig. 5).

The DPCSV responses of these interferents were compared at MIP- and NIP-modified electrodes. In the case of the MIP(Ura)-modified HMDE sensor (Fig. 6(a)), the current response of Ura yielded a quantitative (100%) recovery, while BA, Hx, Ad, and Cy were found to be less responsive. Other interferents, such as Cff, UA, Gu, and 5FU, showed absolutely no response. The NIP-modified HMDE sensor produced an insignificant response for Ura and 5FU but significant affinities for all the interferents when present alone in the test solution (Fig. 6). This revealed that the proposed method is 'system specific,' under the imprinting effect of MIP, responding to the selective binding of the test analyte without contributions from nonspecific bindings. Insofar as the MIP(5FU)-modified HMDE sensor is concerned, 5FU gave a quantitative (100%) recovery, while Ura, Cff, Ad and AA showed extremely poor binding affinities, and BA, Hx, Cy, and Gu showed absolutely no response (Fig. 6(b)).

In the present investigation, purine bases (Ad, Gu, Hx, Cff, and UA) could not fit into binding cavities in the proposed sensors of Ura and 5FU owing to their large sizes. With the MIP(Ura)-based HMDE sensor, it appears that the  $-C=O$  ( $C_4$ ) group of Ura has a distinctive role in the creation of binding specificity, which is absent in Cy. The

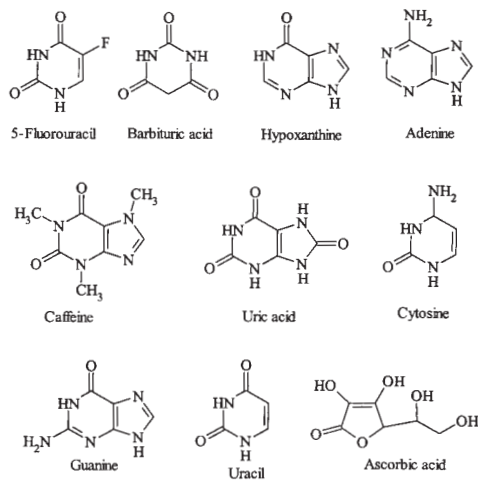


Fig. 5. Chemical structures of uracil, 5-fluorouracil and some cross-reactants.

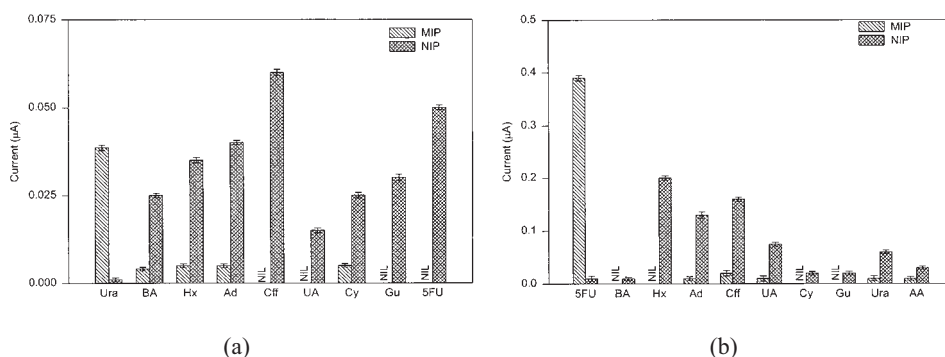


Fig. 6. (a): Sensor response for  $0.00498 \mu\text{g mL}^{-1}$  solution of Ura and its interferences. (b): Sensor response for  $0.0099 \mu\text{g mL}^{-1}$  solution of 5FU and its interferences.

comparatively weaker bases 5FU and BA owing to the presence of electron-withdrawing groups at  $\text{C}_5$  and  $-\text{C}=\text{O}$  at  $\text{C}_4$ , respectively, show no H-bonding comparable to that of Ura. On the other hand, fluorine plays an important role in the formation of binding sites because of its specific hydrogen-bonding interactions with the functional monomers (Fig. 1B), which emerged as a key factor offering marked variation in the sensing ability of the MIP(5FU) vis-a-vis the MIP(Ura)-modified HMDE sensor.

#### 4. Analytical Applications

Once the proposed method was established for aqueous solutions of test analytes, both Ura- and 5FU-imprinted polymer-modified HMDE sensors were subjected to validation for their binding abilities of Ura and 5FU, respectively, in complex matrices of real samples. The blood plasma samples used in this study were appropriately diluted with water (50-fold Ura, 100-fold 5FU), maintained at pH 7.0, and tested for Ura and 5FU without any sample pretreatment. Although dilution helped mitigate the matrix (proteins, anticoagulant species, and other anions) effect, asymmetry in voltammetric peaks is a matter of concern. Nevertheless, this did not vitiate the accuracy of the desired result (Figs. 4A and 4B (g, h)). In fact, the diluted plasma samples were found to be very similar to the diluted aqueous samples in terms of sorption behavior. This was evident from the respective calibration equations and LOD values obtained for blood plasma samples as given below:

(For Ura, present in blood plasma, in concentration range  $0.00049\text{--}0.11736 \mu\text{g mL}^{-1}$ );

- $I_{\text{PC}} (\mu\text{A}) = (7.606 \pm 0.018)C + (0.0002 \pm 0.0005)$ ,  $\nu = 0.99$ ,  $n = 8$

$$\text{LOD} = 0.3 \text{ ng mL}^{-1} (3\sigma, \text{RSD} = 0.3\% \text{ between three sets of LOD data})$$

(For 5FU, present in blood plasma, in the concentration range  $0.00199\text{--}0.0350 \mu\text{g mL}^{-1}$ );

- $I_{PC} (\mu A) = (39.494 \pm 0.199)C + (0.00026 \pm 0.00025)$ ,  $\nu = 0.99$ ,  $n = 7$

$$\text{LOD} = 0.22 \text{ ng mL}^{-1} (3\sigma, \text{RSD} = 0.4\% \text{ between three sets of LOD data})$$

However, it is better to establish a standard curve in the same environment as real samples.

Further validation of the proposed method was performed, employing a standard technique of HPLC measurement.<sup>(38,39)</sup> Although both methods have similar orders of precision within the lower concentration regions studied (Ura: 0.00049–0.11736  $\mu\text{g mL}^{-1}$  and 5FU: 0.00199–0.0350  $\mu\text{g mL}^{-1}$ ) in blood plasma samples (Student's t-test:  $t_{\text{cal}} 1.05 < t_{\text{tab}} 3.18$  for Ura and  $t_{\text{cal}} 0.63 < t_{\text{tab}} 2.57$  for 5FU, confidence level 95%,  $\nu = 0.99$ ), the proposed sensors are apparently more sensitive than the HPLC method [LOD: 0.625  $\text{ng mL}^{-1}$ (Ura), 10  $\text{ng mL}^{-1}$  (5FU)] for Ura and 5FU detections.

## 5. Conclusion

The proposed MIP-modified HMDE sensors for Ura and 5FU have excellent imprinting and sensing abilities for their corresponding templates (test analytes) present in aqueous and complex matrices of blood plasma samples. Both sensors assure reliable detection of Ura and 5FU at trace levels in the blood plasma samples of patients at the primary stage of pyrimidine disorders and are particularly useful for detecting fluoropyrimidine toxicity in cancer treatment. The imprinting versatility of the same MIP motif for both Ura and 5FU is a unique feature of the present investigation.

## Acknowledgement

The support of this work by the Department of Science and Technology, SR/S1/IC-18/2006, is gratefully acknowledged.

## References

- 1 B. Tavazzi, G. Lazzarino, P. Leone, A. M. Amorini, F. Bellia, C. G. Janson, V. D. Pietro, L. Ceccarelli, S. Donzelli, J. S. Francis and B. Giardina: *Clin. Biochem.* **38** (2005) 997.
- 2 B. Bouzid and A. M. G. Macdonald: *Anal. Chim. Acta* **211** (1988) 155.
- 3 B. Bouzid and A. M. G. Macdonald: *Anal. Chim. Acta* **211** (1988) 175.
- 4 J. L. Gao, K. S. Y. Leung, Y. T. Wang, C. M. Lai, S. P. Li, L. F. Hu, G. H. Lu, Z. H. Jiang and Z. L. Yu: *J. Pharm. Biomed. Anal.* **44** (2007) 807.
- 5 P. Wang and J. Ren: *J. Pharm. Biomed. Anal.* **34** (2004) 277.
- 6 R. Horváth, T. Kerékgyártó, G. Csúcs, S. Gáspár, P. Illés, G. Rontó and E. Papp: *Biosens. Bioelectron.* **16** (2001) 17.
- 7 R. N. Goyal, U. P. Singh and A. A. Abdullah: *Indian J. Chem. A* **42** (2003) 42.
- 8 H. Liu, G. Wang, J. Hu, D. Chen, W. Zhang and B. Fang: *J. Appl. Polym. Sci.* **107** (2008) 3173.
- 9 P. A. C. Piunno and U. J. Krull: *Anal. Bioanal. Chem.* **381** (2005) 1004.
- 10 V. Selvaraj and M. Alagar: *Int. J. Pharm.* **337** (2007) 275.

- 11 M. Boisdron-Celle, G. Remaud, S. Traore, A. L. Poirier, L. Gamelin, A. Morel and E. Gamelin: *Cancer Lett.* **249** (2007) 271.
- 12 G. Micoli, R. Turci, M. Arpellini and C. Minoia: *J. Chromatogr. B* **750** (2001) 25.
- 13 D. Anderson, D. J. Ker, C. Blesing and L. W. Seymour: *J. Chromatogr. B* **688** (1997) 87.
- 14 R. Pisano, M. Breda, S. Grassi and C. A. James: *J. Pharm. Biomed. Anal.* **38** (2005) 738.
- 15 M. Khodari, M. Ghandour and A. M. Taha: *Talanta* **44** (1997) 305.
- 16 T. Kobayashi, S. S. Leong and Q. Zhang: *J. Appl. Polym. Sci.* **108** (2008) 757.
- 17 S. L. Xia, H. Y. Wang and T. Kobayashi: *Mater. Res. Soc. Symp. Proc.* **787** (2004) 103.
- 18 A. J. Hall, P. Manesiotis, J. T. Mossing and B. Sellergren: *Mater. Res. Soc. Symp. Proc.* **723** (2002) 11.
- 19 K. Yano, K. Tanabe, T. Takeuchi, J. Matsui, K. Ikebukuro and I. Karube: *Anal. Chim. Acta* **363** (1998) 111.
- 20 B. Sellergren, P. Manesiotis and A. J. Hall: Sweden Patent, WO 2004067578 A1 20040812, 2004.
- 21 H. Y. Wang, S. L. Xia, H. Sun, Y. K. Liu, S. K. Cao and T. Kobayashi: *J. Chromatogr. B* **804** (2004) 127.
- 22 K. Sreenivasan: *React. Funct. Polym.* **67** (2007) 859.
- 23 S. L. Xia, H. Y. Wang, H. Sun, Y. K. Liu and S. K. Cao: *Chin. Chem. Lett.* **14** (2003) 794.
- 24 Q. Zhang, T. Kusunoki, Q. Xu, H. Wang and T. Kobayashi: *Anal. Bioanal. Chem.* **388** (2007) 665.
- 25 C. I. Lin, A. K. Joseph, C. K. Chang and Y. D. Lee: *Biosens. Bioelectron.* **20** (2004) 127.
- 26 A. Kugimiya, T. Mukawa and T. Takeuchi: *Analyst* **126** (2001) 772.
- 27 F. Puoci, F. Iemma, G. Cirillo, N. Picci, P. Matricardi and F. Alhaique: *Molecules* **12** (2007) 805.
- 28 B. Singh and N. Chauhan: *Acta Biomater.* **4** (2008) 1244.
- 29 B. B. Prasad and D. Lakshmi: *Electroanalysis* **17** (2005) 1260.
- 30 D. Lakshmi, B. B. Prasad and P. S. Sharma: *Electroanalysis* **18** (2006) 918.
- 31 H. M. Saffarian, R. Srinivassan, D. Chu and S. Gilman: *J. Electroanal. Chem.* **504** (2001) 217.
- 32 J.-P. Bégué and D. Bonnet-Delpon: *General Remarks on Structural, Physical and Chemical Properties of Fluorinated Compounds: Bioorganic and Medicinal Chemistry of Fluorine* (John Wiley & Sons, Inc., New York, 2008) p. 1.
- 33 D. Hamer, D. M. Waldron and D. L. Woodhouse: *Arch. Biochem. Biophys.* **47** (1953) 272.
- 34 X.-Q. Lin and G.-P. Jin: *Electrochim. Acta* **50** (2005) 3210.
- 35 D. J. Brown: *Heterocyclic Compounds: Thy Pyrimidines* (Interscience, New York, 1994) Vol. 52.
- 36 A. Les and L. Adamowicz: *J. Phys. Chem.* **93** (1989) 7078.
- 37 D. A. Skoog, F. T. Holler and T. A. Nieman: *Principles of Instrumental Analysis*, 5th edn. (Harcourt Brace College Publishers, Florida, 1998) p. 13.
- 38 G. Remaud, M. Boisdron-Celle, C. Hameline, A. Morel and E. Gamelin: *J. Chromatogr. B* **823** (2005) 98.
- 39 W. Wattanatorn, H. L. McLeod, J. Cassidy and K. E. Kendle: *J. Chromatogr. B* **692** (1997) 233.